

Animal Study

e **Transfixation of the Sacroiliac Joint:
Biomechanical Stability of a Dual-Implant
Minimally Invasive Procedure**

Steven M. Falowski, MD¹, and Antonio Valdevit, PhD²

From: ¹Neurosurgical Associates
of Lancaster, Lancaster, PA ²SEA,
Ltd., Columbus, OH

Address Correspondence:
Antonio Valdevit, PhD
SEA, Ltd.,
7001 Buffalo Parkway
Columbus, OH 43229
Email: avaldevit@sealimited.com

Disclaimer: There was no external
funding in the preparation of this
manuscript.

Conflict of interest: Dr. Falowski
is a consultant, research, and
equity for CornerLoc and has
equity in Painteq.

Manuscript received: 06-29-2021
Revised manuscript received:
11-29-2021
Accepted for publication:
01-03-2022

Free full manuscript:
www.painphysicianjournal.com

Background: Despite minimally invasive techniques for sacroiliac joint fixation, clinical challenges remain. The investigators hypothesized the studied technique will transfix the sacroiliac joint to a level comparable to the intact sacroiliac joint.

Objectives: The study objective was to determine the dynamic stability of a square inter-joint implant using a triangular notch in opposing bone segments spanning the joint space.

Study Design: Stability was assessed by measuring micromotion using contralaterally placed transducers spanning the sacroiliac joint of a specimen during cyclic loading.

Setting: A porcine in-vitro model was equipped with micromotion transducers on the intact and surgically implanted sacroiliac joint. Cyclic loading was applied on the L4 vertebra and the recorded micromotion data at each sacroiliac joint was analyzed.

Methods: Porcine specimens from L3 to the sacrum including the pelvic ring were used to biomechanically evaluate the implantation technique. A novel technique consisting of a square inter-joint implant was placed so as to create a triangular stabilization notch within adjacent bony components of the sacroiliac joint. Displacement transducers were placed across implanted and contralateral porcine sacroiliac joint. Specimens were subjected to compressive loading between -10N and -100N followed by bending/rotation between 0.4Nm and 4.0Nm. Tests were conducted at 0.5Hz for 200 cycles. For each loading mode, transducer deflections (or rotations) were averaged at five-cycle intervals. Student's t-tests were used to compare fitted parameters between implanted and intact sacroiliac joint.

Results: In compression, implanted SIJ displayed reduced deflection compared to intact sacroiliac joint ($P < 0.0001$). In bending/rotation, initial rotation for the intact sacroiliac joint was increased compared to implanted sacroiliac joint ($P < 0.0001$). The computed Half-Life parameter represents the number of cycles at which the initial rotation decreases by 50% and was found to be statistically reduced for implanted sacroiliac joint as compared to intact sacroiliac joint.

Limitations: The use of porcine specimens resulted in uniform and good quality bone purchase. Further study may be required to evaluate the technique in older patients where bone quality is reduced.

Conclusions: Compared to the intact sacroiliac joint, the implant and procedure in this study demonstrated decreased motion under cyclic compression. Under rotation, the implanted sacroiliac joint displayed increased initial stability that subsequently normalized to intact sacroiliac joint values.

Key words: Transfixation, Minimally invasive, Sacroiliac Joint, Micromotion, Biomechanics, Dynamic Loading, Stability, In-Vitro

Pain Physician 2022; 25:E469-E479

Sacroiliac joint fixation has historically been an open and relatively invasive procedure. With the advent of recent minimally invasive techniques, outcomes have improved, and morbidity has declined (1). Despite these advances, clinical challenges in treatment remain. Among the limitations to sacroiliac joint treatment is an appropriate diagnosis. Often, low back pain is attributed to the involvement of the hip, lumbosacral spine, or the sacroiliac joint in some combination. Diagnosing the sacroiliac joint in isolation is considered only after involvement of other anatomic sites has been ruled out. Furthermore, surgical intervention is considered after failure of conservative treatment.

Current minimally invasive techniques involve the use of screw or porous implant fixation. There are several concepts with regards to the manner for optimal surgical placement of transarticular screw fixation devices (2). Accepted techniques for fixation include fixation across the joint via a lateral or posterior-oblique approach, as well as graft insertion via a direct posterior approach. Biomechanical studies have investigated both the number of devices, device trajectory, and geometry (3). These studies have focused upon the issue of stability of the sacroiliac joint under static loading conditions as in a single leg stance protocol. In evaluating stability, loading is often applied until fracture of the specimen is achieved. Subsequent analysis computing the deformation or stiffness of the construct is then compared among the various instrumentation systems to arrive at a maximum stiffness or minimal deformation construct (4). The limitation of such testing regimens stems from the lack of dynamic response of the instrumentation under cyclic loading. All instrumentation will limit movement following destabilization. The clinical question of importance rests with the dynamic response of the specimen/instrumentation composite to cyclic loading and whether immediate stable fixation can be attained or if equilibration to a stable configuration that will not unduly stress shield the sacroiliac joint is possible. In one of the few studies examining the effects of unilateral fixation upon the contralateral sacroiliac joint, Lindsey et al found non-significant biomechanical effects due to unilateral fixation when conducting static testing (5). If the use of unilateral fixation is to provide more clinically relevant ramifications, such clinical scenarios can only be addressed through the use of cyclic dynamic loading protocols.

Many *in vitro* studies employ optimal markers for tracking 3-dimensional (3D) sacroiliac joint motion

under loading. The application of multiple directional loading through the use of optical tracking methods provides 3D motion data. Such testing configurations can yield large errors associated with the motion of the sacroiliac joint (6,7). While such methods have proven viable for analysis of large motions as seen in hips and knees, the motion of the sacroiliac joint is subtle and is further reduced with surgical intervention. Furthermore, optical techniques are limited if one is to study cyclic motion. The use of mechanical data acquired through material testing machine actuators and load cells are masked by inherent motion within the lumbosacral spine (4). Localized motion can be directly measured through linear variable differential transformers (LVDTs) or differential variable reluctance transducer (DVRT) devices across the region of interest (8). Regardless of the sacroiliac joint motion measurement technique, the application of continuous cyclic loading versus multiple single cycle static loading represents a more clinically relevant instrumentation performance scenario (9,10).

The current study addresses the use and functionality of a novel intra-articular implant that stabilizes the sacroiliac joint by pinning both the sacrum and ilium. Transfixation across the sacroiliac joint is achieved by imparting a square implant with unidirectional teeth whereby the corners engage both the sacrum and ilium via 2 triangular notches in each bone segment to accommodate a rectangular implant that spans the sacroiliac joint. Two such devices are placed perpendicular to each other, establishing a convergence. The goal of the current study is to determine if such a minimally invasive surgical procedure can provide sufficient fixation across the sacroiliac joint by a resulting pinning effect due to the rectangular shape of the device and the unidirectional teeth. The investigators hypothesized that such a technique would stabilize the sacroiliac joint by creating triangular notches in the bone segments to accommodate the rectangular implant spanning the sacroiliac joint. It is further hypothesized that such a configuration will lead to initial stability and result in comparable stability to the native contralateral sacroiliac joint after cyclic loading due to implant settling within the joint space.

METHODS

The mechanical advantages connected with animal models stem from reproducible geometry and increased uniform bone mineral density between specimens. Furthermore, the availability of animal speci-

mens is significantly increased as compared to human specimens. Aside from the availability, the mechanical integrity associated with human specimens is generally classified as osteopenic or osteoporotic. A viable alternative to the use of human samples is the employment of suitable animal analogs. Many studies employing human specimens are predominantly confined to single or several static loading cycles. In the case of the current study, the use of repeated loading may lead to specimen degradation. The use of a porcine specimen where the bone density is both consistent and of improved mechanical quality compared to a human pelvis facilitated the application of continuous fatigue loading. The authors recognize that while quadrupeds display different biomechanical properties compared to humans, the current study was designed to examine the effects of the instrumentation as compared to the contralateral intact sacroiliac joint. It is recognized that the biomechanics manifested by quadrupeds is different from human bipedal motion. Despite this difference, selection of an appropriate animal model was feasible in light of the specific *in vitro* test cyclic requirements for this study. Institutional Review Board/Research Ethics Committee approval was not applicable for this study as porcine specimens were used for biomechanical testing and were acquired from a certified supplier.

The investigators performed a bilateral comparison for fixation in an effort to investigate stability and comparison to a normal joint. The basis of the implant stability stems from cortical engagement and retainment of ligamentous compression to provide rectangular pinning across the sacroiliac joint. Diseased joints can vary in presentation of pathology. Using our models as their own controls permits the comparison between an unaltered native intact sacroiliac joint to the contralateral implanted sacroiliac joint. Clinically one can extrapolate that the relative differences would be exacerbated in a diseased joint. Pilliar et al, using a canine model, described the presence of micromotion on the order of 28 μm can result in bone ingrowth while movement in excess of 150 μm generates implant attachment via connective tissue (11).

That is, there is a level of micromotion that can benefit bone remodeling. Conversely, overly rigid constructs can contribute to stress shielding. Engh et al, in examining the effects of implanted porous-coated anatomic medullary locking prostheses post-mortem, concluded that strain shielding was associated with bone remodeling changes that resulted in regional

reductions in bone mineral content that ranged from 7% to 78% (12).

The shielding of the surrounding bone by the implant results in reduced strength reduction in accordance with Wolff's Law as localized bone loading is reduced. In the current study, the clinical concerns of both insufficient and excessive micromotion were addressed. Micromotion was observed between 64 μm and 49 μm for the intact and implanted sacroiliac joint, respectively. The scale of the measurements indicates that while the model may differ from that of a human subject, the relative implications can be inferred. The anatomical variation from human anatomy is less crucial, and the use of reproducible and viable anatomic mechanical integrity provides the rationale for employment of porcine specimens. Such a model is not unique for the investigation of the pelvis and sacroiliac joint for *in vitro* testing (13-15). In the removal of soft tissue, specimens lose a significant portion of their mechanical stability as compared to the *in vivo* condition. The use of an intact contralateral comparison was to evaluate if the applied instrumentation could initially stabilize and subsequently maintain the stability at a level that is comparable to an intact joint. The application of any instrumentation to a joint or fracture can run the risk of generating an overly stiff construct which may be subsequently susceptible to stress shielding and thus, possibly create a situation of a delayed or nonunion scenario. The subsequent investigation regarding the settling of instrumentation to a level that is comparable to an intact contralateral sacroiliac joint is of benefit as compared to an overly stiff construct that can lead to altered biomechanics. To accommodate the smaller porcine pelvis, the smallest implants were employed in this study. Seven porcine segments from L3 to the mid femur were obtained from fully mature, 125 kg animals (Animal Technologies, LLC., Tyler, TX). The ligamentous tissues across the sacroiliac joint were preserved. One randomly selected sacroiliac joint was visualized using syringe needles, and location was verified under fluoroscopy. Two devices (CornerLoc., Tulsa, OK) were implanted to stabilize the sacroiliac joint per the surgical procedure (Fig. 1).

Measurement of Sacroiliac Joint Motion

The localized motion of the intact and implanted sacroiliac joint cannot be recorded by the actuator of the testing machine itself, as the actuator will only record the total motion associated with the sacroiliac joint and the lumbosacral spine. While there are

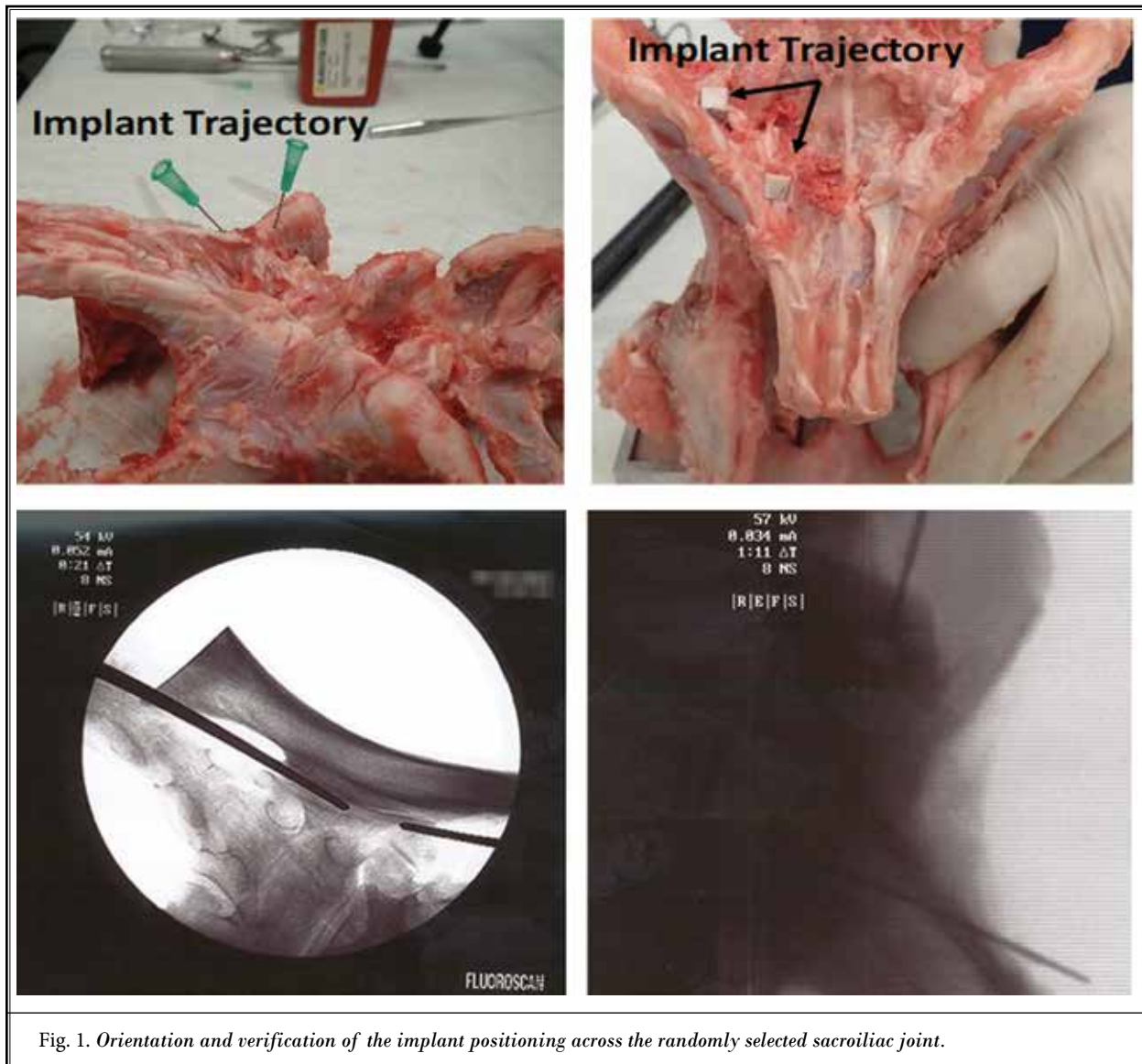


Fig. 1. Orientation and verification of the implant positioning across the randomly selected sacroiliac joint.

several studies that have employed optical methods, the use of triad reflective markers in such small geometries can be problematic. In the current study, displacement transducers capable of micron resolution were employed. These transducers have been previously used in other studies and display an accurate linear response with respect to applied deformation. While the use of LVDTs is a viable alternative to the transducers employed in this study, they suffer from the fact that they must be used in an exact linear, uniaxial configuration. Any deviation from the central axis can damage or alter the transducer response. A custom-designed strain gauge-based displacement

transducer was fabricated and calibrated to record endplate movement under cyclic loading of the joint periphery. The transducer records changes in displacement through a strain gauge mounted at the apex of a flexible central arc (Fig. 2, Left). When the relative separation distance between the tabs of the transducer is altered due to tension or compression, a corresponding increase or decrease in the arc diameter is generated and results in the deformation of the strain gauge located at the apex of the arc (16,17).

Using a Wheatstone bridge circuit and amplifier, the gauge resistance change was transformed to an output voltage that was subsequently converted to

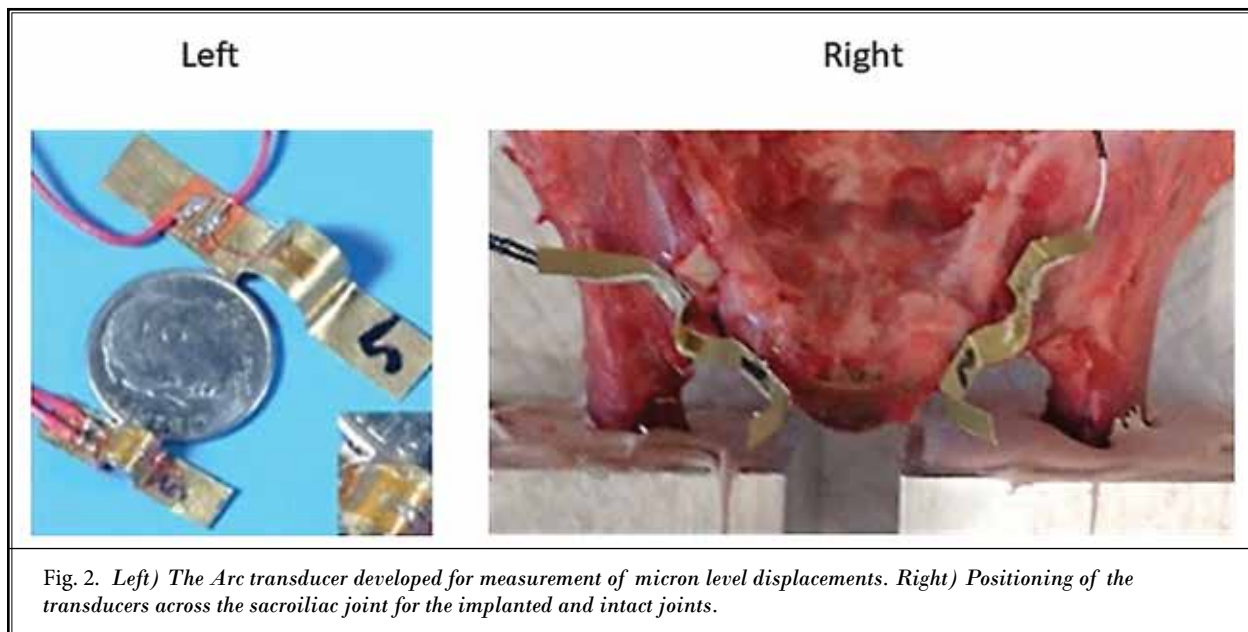


Fig. 2. Left) The Arc transducer developed for measurement of micron level displacements. Right) Positioning of the transducers across the sacroiliac joint for the implanted and intact joints.

a known displacement using a previously generated calibration curve between the transducer output voltage and the change in tab separation distance as measured with a micrometer. Prior to use, the transducer and accompanying electronics were allowed to equilibrate in the laboratory environment for a minimum of 20 minutes. Following implantation of the rectangular pinning devices, the transducer was placed across the implanted and contralateral sacroiliac joint at the same relative location (Fig. 2, Right). Therefore, all factors were kept constant on both sides, with the exception of the procedure performed on the treated side.

Specimen Loading

Specimens were embedded in resin for integration into the materials testing machine. The superior aspect of L3 and each distal portion of the ilium were embedded (Fig. 3, Left). Specimens were subjected to compressive loading between -10 N and -100 N at a rate of 0.5 Hz for 200 cycles. Load versus deformation data from the materials testing machine (TA Instruments, ElectroForce 3300, Eden Prairie, MN) and transducer deflections from each sacroiliac joint were acquired at a rate of 40 Hz using a data acquisition system (DI-155 HS, Dataq Instruments, Akron, OH). The placement of the transducer at L4 was to establish if the linearity between the applied motion of the testing machine piston was being directly transferred to the specimen. During cyclic loading of biological tissue, the loading

applied by the testing frame may result in a lag in specimen loading due to viscoelastic effects of soft tissues such as the intervertebral discs. By placing a transducer across L4, the authors were able to ensure that during testing, viscoelastic effects were minimal. That is, the specimen loading response was essentially linear with respect to the load application. The transducers across the sacroiliac joint were oriented so as to monitor motion across and parallel to the sacroiliac joint where the implantation was performed. The contralateral intact side received transducers in a similar orientation and position.

Following compressive testing, specimens were re-embedded to allow for bending/rotation of the sacroiliac joint. The anterior aspect of each ilium was embedded in an aluminum sleeve. (Fig. 3, Right). The loading point was located on the midline of the sacrum at a distance of 40mm from the center of the lateral aspect sacroiliac joint. Loading parameters for the testing machine were identical to those for compression testing. The resulting moment arm facilitated bending between 0.4 nm and 4.0 nm. Data were acquired as previously described. For each loading mode, the maximum and minimum deflections at each cycle were extracted and averaged for every 5-cycle interval. In the case of bending/rotation, the deflections were converted to angle measurements through trigonometric identity. The mean deflections for the respective sacroiliac joint condition were averaged across the respective cycle number for each loading mode.

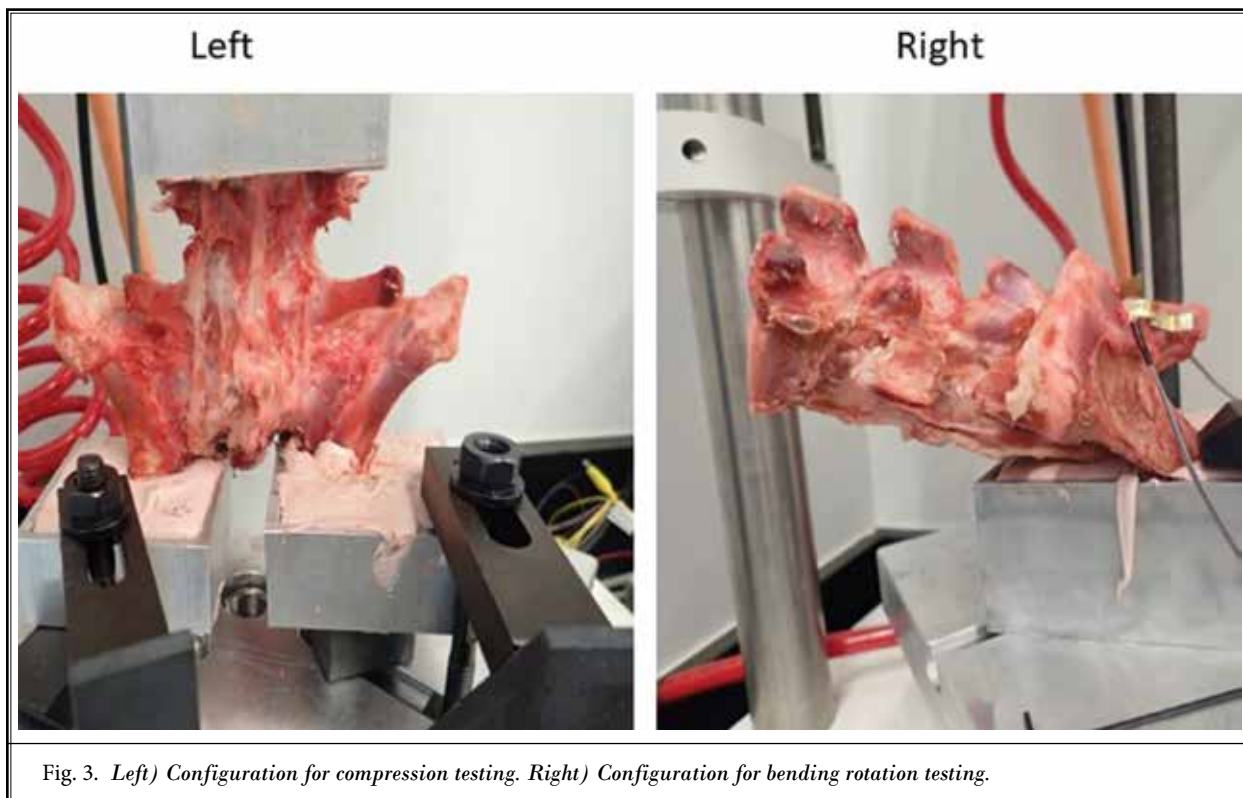


Fig. 3. *Left*) Configuration for compression testing. *Right*) Configuration for bending rotation testing.

Statistical Methods

Under the compressive loading, both the implanted and intact sacroiliac joints were relatively stable over the number of cycles applied. As such, a horizontal line regression was used to fit the data (Prism 7.0 GraphPad, Inc., San Diego, CA). A Student's t-test was used to compare the deflections of the implanted and intact sacroiliac joint. Under bending/rotation loading, both the implanted and intact sacroiliac joint displayed a nonlinear response with respect to the number of applied cycles. Nonlinear exponential regression was used to fit the observed rotation of each sacroiliac joint to the number of cycles applied (Prism 7.0 GraphPad, Inc., San Diego, CA). Parameters of the exponential function are identified by Y_0 (the initial position), K (the rate of change), $Span$ (the total change), and $Plateau$ (the asymptotic limit of the subsidence) (Fig. 4). A Student's t-test was used to compare the resulting curve parameters for the implanted and intact sacroiliac joint.

RESULTS

The resulting data are based upon 7 compression specimens and 6 bending/rotation specimens. One specimen was damaged during removal from the

embedding material following compression testing. Embedding of this specimen was attempted but was unsuccessful.

Transducer Calibration

All transducers display linear response between the output voltage of the circuitry in the applied displacement between the mounting tabs of the transducers (Fig. 5). The R-squared value for the linear regression of output voltage and applied displacement exceeded 0.99 for all transducers. Transducers 1 and 2 were used throughout the testing and were not damaged during application between specimens.

Cyclic Compression

The statistical analysis software selected a horizontal line fit to each data set compared to a straight line fit (F test, $P > 0.5$). The cyclic compression data and the fitted horizontal line for the implanted and intact sacroiliac joint are seen in Fig. 6, Left and Fig. 6, Right, respectively. Under cyclic compression, the intact sacroiliac joint displayed a deflection of $0.064 (\pm 0.001)$ mm as compared to a deflection of $0.049 (\pm 0.001)$ mm for the implanted sacroiliac joint. This difference was statistically significant ($P < 0.0001$). For both tests, the

fitting residuals were normally distributed about the horizontal line ($P > 0.5$ for both sets).

Cyclic Bending/Rotation

The statistical analysis software selected a single decay curve for both data sets as compared to a straight line fit (F test, $P > 0.5$, Fig. 7). The R-squared value for both data sets was in excess of 0.86. The initial value of the rotation (Y_0) for the intact sacroiliac joint was $0.867 (\pm 0.002)^\circ$ as compared to the implanted sacroiliac joint value of $0.821 (\pm 0.001)^\circ$ (Fig. 8, Left, $P < 0.0001$). At the termination of the test, the observed rotation (Plateau) was not statistically significant between the intact and implanted sacroiliac joint (Fig. 8, Right, $P > 0.6$) due to the nature of the decay curves associated with both data sets. The exponential fitting process computes the rate associated with exponential defined by the parameter K. It is often more easily interpreted when the associated half-life is reported. Half-life is computed as $(\ln 2/K)$ and represents the number of cycles at which the initial rotation has decreased by 50%. In Fig. 8, bottom, the half-life of the implanted sacroiliac joint is $70 (\pm 8)$ cycles as compared to the half-life of the intact sacroiliac joint, $150 (\pm 28)$ cycles. This difference was statistically significant ($P < 0.02$).

The application of mechanical loading to failure of the surgical construct does not represent a clinically viable scenario unless one is focused on the effects due to traumatic loading. The current study investigated the response to cyclic loading of the sacroiliac joint in the stabilized and intact conditions. Using custom fabricated and calibrated transducers mounted directly across both sacroiliac joints, we were able to measure micromotion across the respective joints under cyclic loading. The implanted sacroiliac joint displayed decreased deflection as compared to the contralateral intact sacroiliac joint under compressive loading through the cyclic loading regimen. The difference was statistically significant ($P < 0.0001$).

Under cyclic bending, the implanted and intact sacroiliac joint displayed a nonlinear exponential decrease in rotation during the loading regimen.

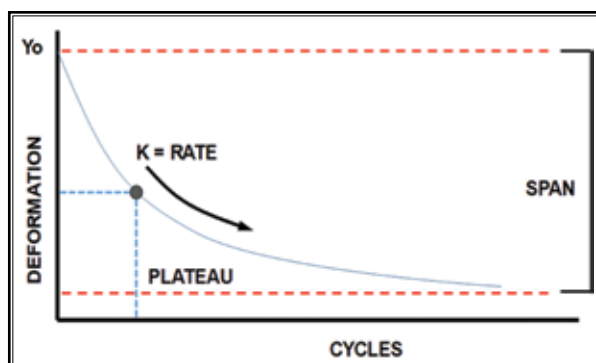


Fig. 4. Schematic of the nonlinear exponential function used to fit the bending/rotation cyclic data.

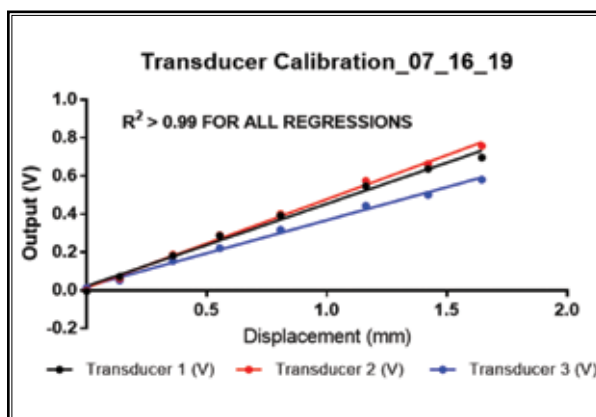


Fig. 5. Results of Arc transducer calibration.

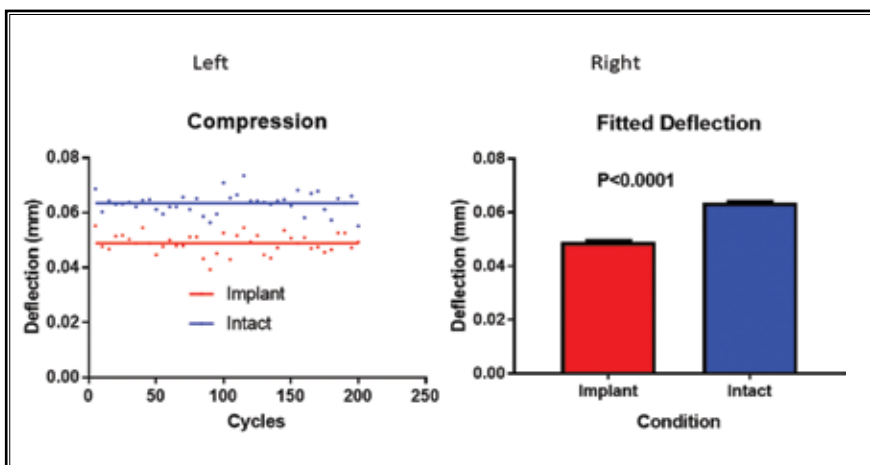


Fig. 6. Left) Plot of compression data for the implanted (Red) and intact (Blue) sacroiliac joint. Right) Fitted deflection (via horizontal line) for the Implanted (Red) and Intact (Blue) sacroiliac joint. The implanted sacroiliac joint was statistically reduced as compared to the intact sacroiliac joint.

Analysis of the fitted parameters permitted investigation into the response of the implanted and intact sacroiliac joint due to cyclic bending loads. The difference in initial rotational stability, designated as Y_0 , was on the order of 0.05° . While this value may not be sub-

stantial, it was statistically decreased for the implanted sacroiliac joint as compared to the contralateral intact joint ($P < 0.001$). This is not unexpected as one would expect that implantation of a device spanning the joint would lead to initial increased stability as compared to the intact condition.

The total change in rotational stability for the implanted sacroiliac joint over the number of loading cycles was 0.07° as compared to 0.14° for the intact sacroiliac joint ($P < 0.002$), while the asymptotic limit (Plateau) was not statistically different ($P < 0.6$) between intact and implanted sides of the sacroiliac joint. It is important to note that while the implantation of the device leads to a more stable configuration than the intact sacroiliac joint (by acting as a press-fit pin between the bone segments across the sacroiliac joint), the subsequent effects of cyclic loading served to settle and seat the implanted sacroiliac joint to a level that is comparable and not statistically different from the native sacroiliac joint. Such a scenario can be extrapolated to the clinical condition where an overly stiff sacroiliac joint construct can lead to stress shielding of the implanted joint and impart altered mechanical and physiological loading conditions upon the contralateral intact sacroiliac joint. The use of triangular implants

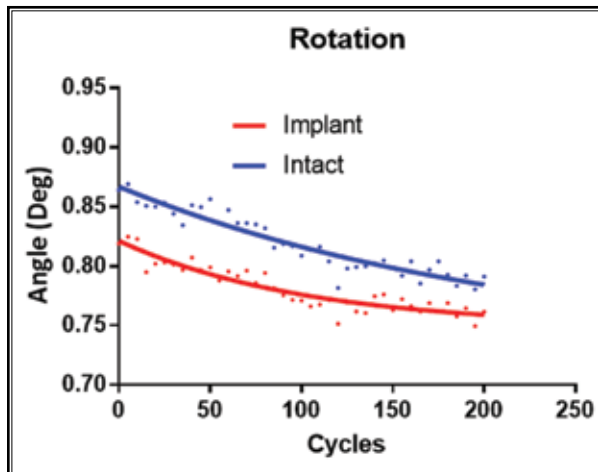


Fig. 7. Plot of the Rotation data under cyclic load for the Implanted (Red) and Intact (Blue) sacroiliac joint. Both sacroiliac joints displayed a nonlinear response versus applied cycles.

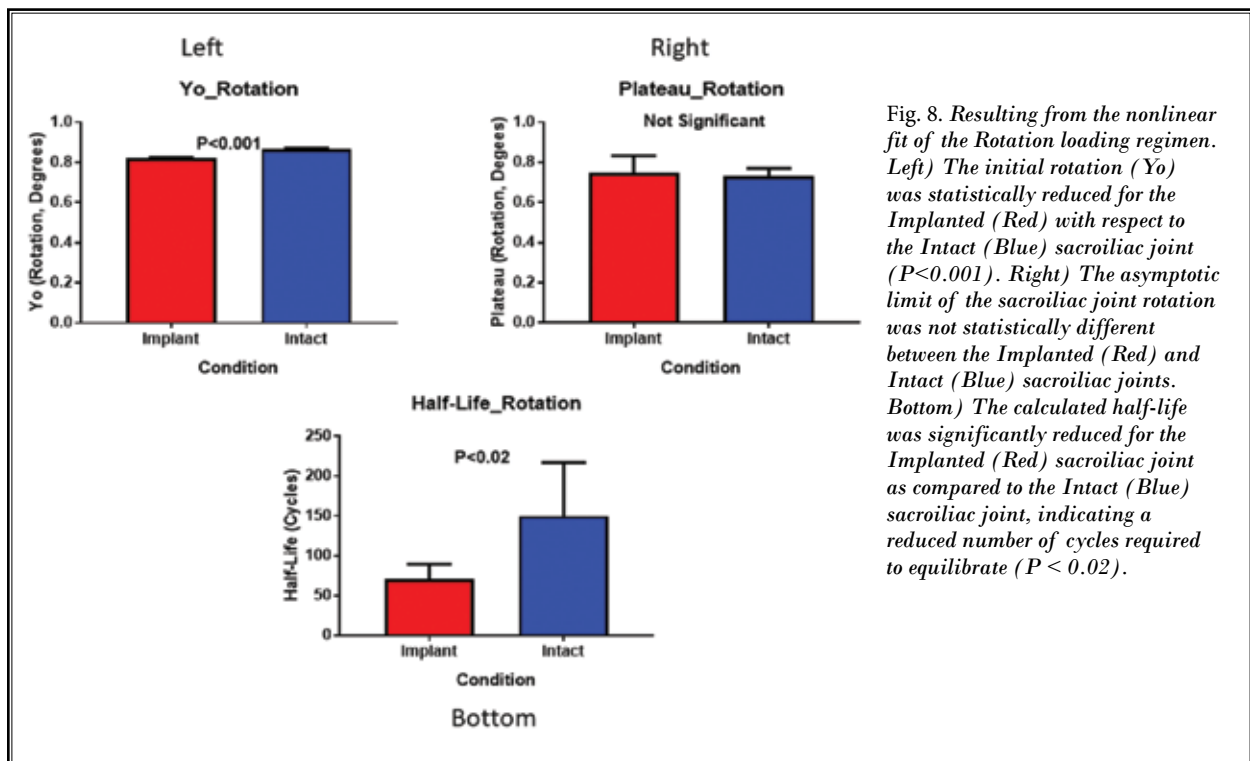


Fig. 8. Resulting from the nonlinear fit of the Rotation loading regimen. Left) The initial rotation (Y_0) was statistically reduced for the Implanted (Red) with respect to the Intact (Blue) sacroiliac joint ($P < 0.001$). Right) The asymptotic limit of the sacroiliac joint rotation was not statistically different between the Implanted (Red) and Intact (Blue) sacroiliac joints. Bottom) The calculated half-life was significantly reduced for the Implanted (Red) sacroiliac joint as compared to the Intact (Blue) sacroiliac joint, indicating a reduced number of cycles required to equilibrate ($P < 0.02$).

has been examined by Panico et al who examined the application of these devices and reported that they might be employed as a supplement to rod/screw systems when they provide a protective effect to the construct (18). In this study, the use of a rectangular implant within opposite triangular notches across the sacroiliac joint was examined in isolation to evaluate resultant sacroiliac joint stability under cyclic loading. Cross III et al noted extrusion of intra-articular material from the joint capsule during trans-articular screw compression (19). In this study, the implanted sacroiliac joint transitioned to comparable rotational motion to the intact sacroiliac joint during the cyclic loading under bending conditions. It therefore maintains normal physiologic movement.

While the initial and final rotational stability can be of biomechanical importance, of clinical relevance may be the data associated with the dynamic response of the implanted and intact sacroiliac joint. This parameter is represented by the rate or K value, of the non-linear exponential fitted curve to the data. Although this parameter is commonly used to evaluate dynamic response, in light of this study, it may be more clinically relevant to the present rate as half-life, thereby representing the number of loading cycles required to achieve a 50% decrease from the initial rotational motion. Conventionally, equilibrium is established at a value of 5 half-lives. In this study, the implanted sacroiliac joint displayed a half-life value of 71 cycles as compared to a value of 150 cycles for the intact sacroiliac joint. This difference was statistically significant ($P < 0.02$). Using the 5 half-lives convention for equilibrium, this would compute to achievement of rotational equilibrium for the implanted sacroiliac joint at 355 cycles as compared to 750 cycles for the intact sacroiliac joint. Clinical interpretation of the half-life would be the "settling" of the implant construct. Ideally, it would be desirable to have a rapid settling configuration so as to enable healing to occur. Delayed equilibrium could prolong the time required for a stable sacroiliac joint and hence may delay union due to continuous settling and/or migration.

Biomechanical studies involving human specimens have been loaded to 7.5 nm (7,17). Under these loading conditions and employing optical tracking, Jeong et al reported single-plane rotation of $4.5 (\pm 3.3)^\circ$ for nutation-counterrotation. In this study, a loading moment of 4.0 nm was applied (7). Extrapolating the angular rotations observed in the current study results in the initial (Y_0) values of rotation of the intact and implanted

sacroiliac joint of 1.6° and 1.5° , respectively, for flexion. With a 7.5 nm applied moment, Cross III et al reported flexion-extension rotations of $2.92 (\pm 0.74)^\circ$ and $1.75 (\pm 0.99)^\circ$ for the intact and instrumented sacroiliac joint using a lag screw/washer configuration in conjunction with a single transarticular screw (19). These rotational results are comparable to those reported for an intact normal density Finite Element Analysis model proposed by Dubé-Cyr et al under flexion-extension $3.86 (\pm 1.60)^\circ$ when loading was applied through the sacrum (20). These values compare favorably to the values in this study when extrapolated to the increased loading level. A study conducted by Dujardin et al employed a loading regimen of 350 N to apply loading across the sacroiliac joint (8). The investigators reported intact pelvis values of from 0.24° to 1.92° for rotation and 0.22 mm to 0.35 mm in displacement. Extrapolating the 100 N compressive load in the current study to the load used in the study by Dujardin results in the intact sacroiliac joint displaying a compression of 0.22 mm and a rotation of 3° . It is noteworthy that Dujardin et al employed LVDT devices to record the micromotion of the sacroiliac joint during loading. Unlike the current study, cyclic loading was not conducted. Despite the reducing loading condition under cyclic loading, the initial values for both intact and pinned sacroiliac joint motions are comparable to those displayed by other biomechanical studies in the literature employing high loads combined with human specimens under static conditions using only several cycles. Zderie et al employed an 80 N starting load with force rate loading rates of 0.01 N/cycle and a 5 nm static torsional load to examine effects of sacroiliac joint fixation. At 1000, 3000, and 5000 cycles the applied loads were 90 N, 100 N, and 130 N, respectively. The flexion rotations for the 7.3 mm cannulated screw and 13 mm washer, screw-in-screw, and transsacral instrumentation at 1000 cycles were 0.76° , 2.12° , and 0.76° , respectively. At the 3000 cycle or 90 N loading level, the corresponding values increased to 2.68° , 3.44° , and 1.3° for the cannulated screw, screw-in-screw, and trans-sacral conditions (21). In the current study, the Initial (Y_0) and Final (Plateau) values for rotation were both less than 1° for the intact and rectangular implant stabilized sacroiliac joint.

Limitations

There are limitations with respect to the current study. The loading conditions of a 100 N force are substantially reduced as compared to other studies. The rationale for this load was 2-fold. The cyclic load-

ing conditions associated with both compressive and rotational bending placed specimens under dynamic loading could result in specimen degradation at higher load levels. The removal of associated musculature surrounding the pelvis considerably reduces the load-bearing capacity of the specimens. The reduced loading facilitated the likelihood of specimens completing the 2 loading regimens to the number of cycles administered. The second reason for the reduced load was associated with the use of porcine specimens, which are reduced in size. Balancing the reduced load used in the study due to porcine specimens is the reproducible and consistent geometry and bone quality associated with the porcine samples. Another limitation as compared to other studies of the sacroiliac joint was the motion, and only one plane was recorded. Other studies examining sacroiliac joint motion use optical methods to obtain 3D motion. While this study only considered motion along or across the sacroiliac joint, the transducers employed were able to measure these respective motions directly as the applied loading was in one plane. Despite these limitations, when the applied loading conditions were extrapolated to those using human specimens, compa-

able results were obtained for resultant motion. Such a comparison provides a measure of confidence for the use of porcine specimens in future studies.

CONCLUSIONS

Considering both biomechanics and physiology, in order to achieve union across the sacroiliac joint, a balance of both stability and a degree of dynamic micromotion is desirable. The implant procedure employed in this study demonstrated statistically decreased motion under cyclic compression as compared to the intact sacroiliac joint. Under rotation, the implanted sacroiliac joint displayed initial increased rotational stability as compared to the intact sacroiliac joint. During rotation, the implanted sacroiliac joint demonstrated a more rapid rate to equilibrium as compared to the intact joint. At the termination of cyclic rotation, the rotational stability of the implanted and intact sacroiliac joint was comparable. The ability of the implant and associated inter-joint pinning process to stabilize and not impart altered biomechanics upon the contralateral joint is important in considering clinical ramifications of sacroiliac joint fixation.

REFERENCES

1. Miller LE, Block JE. Minimally invasive arthrodesis for chronic sacroiliac joint dysfunction using the SImmetry SI Joint Fusion system. *Med Devices (Auckl)* 2014; 7:125-130.
2. Whang P, Cher D, Polly D, et al. Sacroiliac joint fusion using triangular titanium implants vs. non-surgical management: six-month outcomes from a prospective randomized controlled trial. *Int J Spine Surg* 2015; 9:6.
3. Mears SC, Sutter EG, Wall SJ, Rose DM, Belkoff SM. Biomechanical comparison of three methods of sacral fracture fixation in osteoporotic bone. *Spine (Phila Pa 1976)* 2010; 35:E392-E395.
4. Kemper AR, McNally C, Duma SM. Dynamic compressive response of the human pelvis axial loading of the sacroiliac joint. *Biomed Sci Instrum* 2008; 44:171-176.
5. Lindsey DP, Parrish R, Gundanna M, Leasure J, Yerby SA, Kondrashov D. Biomechanics of unilateral and bilateral sacroiliac joint stabilization: laboratory investigation. *J Neurosurg Spine* 2018; 28:326-332.
6. Shih YC, Beaubien BP, Chen Q, Sembrano JN. Biomechanical evaluation of sacroiliac joint fixation with decortication. *Spine J* 2018; 18:1241-1249.
7. Jeong JH, Leasure JM, Park J. Assessment of biomechanical changes after sacroiliac joint fusion by application of the 3-dimensional motion analysis technique. *World Neurosurg* 2018; 117:e538-e543.
8. Dujardin FH, Roussignol X, Hossenbaccus M, Thomine JM. Experimental study of the sacroiliac joint micromotion in pelvic disruption. *J Orthop Trauma* 2002; 16:99-103.
9. Camino Willhuber G, Zderic I, Gras F, et al. Analysis of sacro-iliac joint screw fixation: does quality of reduction and screw orientation influence joint stability? A biomechanical study. *Int Orthop* 2016; 40:1537-1543.
10. Lindsey DP, Perez-Orribo L, Rodriguez-Martinez N, et al. Evaluation of a minimally invasive procedure for sacroiliac joint fusion - an in vitro biomechanical analysis of initial and cycled properties. *Med Devices (Auckl)* 2014; 7:131-137.
11. Pilliar RM, Lee JM, Maniopoulos C. Observations on the effect of movement on bone ingrowth into porous-surfaced implants. *Clin Orthop Relat Res* 1986; 208:108-113.
12. Engh CA, O'Connor D, Jasty M, McGovern TF, Bobyn JD, Harris WH. Quantification of implant micromotion, strain shielding, and bone resorption with porous-coated anatomic medullary locking femoral prostheses. *Clin Orthop Relat Res* 1992; 285:13-29.
13. Kaye EA, Maybody M, Monette S, Solomon SB, Gulati A. Ablation of the sacroiliac joint using MR-guided high intensity focused ultrasound: a preliminary experiment in a swine model. *J Ther Ultrasound* 2017; 5:17.
14. Indahl A, Kaigle A, Reikerås O, Holm S. Sacroiliac joint involvement in activation of the porcine spinal and gluteal musculature. *J Spinal Disord* 1999; 12:325-330.
15. Sussman JS, Sponseller PD, Gearhart JP, Valdevit AD, Kier-York J, Chao EY. A comparison of methods of repairing the symphysis pubis in bladder exstrophy by tensile testing. *Br J Urol* 1997; 79:979-984.

16. Valdevit A, Kambic H, Elster T, El-Said A, inventors; The Cleveland Clinic Foundation, assignee. Displacement Transducer. United States Patent US 6,810,753 B2A. Nov 2, 2004.
17. Valdevit A, Kedzierska A, Gallagher MB, Schneider JM, Ullrich PF. Endplate deformation due to open and strutted intervertebral devices. *Int J Spine Surg* 2019; 13:522-530.
18. Panico M, Chande RD, Lindsey DP, et al. The use of triangular implants to enhance sacropelvic fixation: a finite element investigation. *Spine J* 2020; 10:1717-1724.
19. Cross WW III, Berven SH, Slater N, Lehrman JN, Newcomb AGUS, Kelly BP. In vitro biomechanical evaluation of a novel, minimally invasive, sacroiliac joint fixation device. *Int J Spine Surg* 2018; 12:587-594.
20. Dubé-Cyr R, Villemure I, Arnoux PJ, Rawlinson J, Aubin CÉ. Instrumentation of the sacroiliac joint with cylindrical threaded implants: A detailed finite element study of patient characteristics affecting fixation performance. *J Orthop Res* 2021; 39:2693-2702.
21. Zderic I, Wagner D, Schopper C, et al. Screw-in-screw fixation of fragility sacrum fractures provides high stability without loosening-biomechanical evaluation of a new concept. *J Orthop Res* 2021; 39:761-770.

